Nanoscale

REVIEW

View Article Online
View Journal | View Issue

Check for updates

Cite this: *Nanoscale*, 2023, **15**, 8491

# *In vivo* applications of micro/nanorobots

Cagatay M. Oral [a] and Martin Pumera *[a,b]

Received 2nd February 2023,
Accepted 18th April 2023

DOI: 10.1039/d3nr00502j

rsc.li/nanoscale

Untethered robots in the size range of micro/nano-scale offer unprecedented access to hard-to-reach areas of the body. In these challenging environments, autonomous task completion capabilities of micro/nanorobots have been the subject of research in recent years. However, most of the studies have presented preliminary *in vitro* results that can significantly differ under *in vivo* settings. Here, we focus on the studies conducted with animal models to reveal the current status of micro/nanorobotic applications in real-world conditions. By a categorization based on target locations, we highlight the main strategies employed in organs and other body parts. We also discuss key challenges that require interest before the successful translation of micro/nanorobots to the clinic.

Published on 27 April 2023. Downloaded on 4/10/2026 3:20:11 AM.

## 1. Introduction

In 1966, as an early demonstration of tiny machines in bioengineering, a science fiction movie (*Fantastic Voyage*) depicted the idea of shrinking a submarine and its expedition team for blood clot removal in a nearly dying scientist's carotid artery.[1] Although this revolutionary idea was out of reach until recently, developments in small-scale fabrication techniques and wireless actuation methods have enabled implementation of the concept -swallowing a surgeon- in real-world conditions.[2] Nowadays, the tiny surgeons are known as "micro/nanorobots".

As small-scale objects (ranging from hundreds of micrometers to tens of nanometers), micro/nanorobots hold capabilities to conduct functional operations with semi or full autonomy in hard-to-reach areas of the body.[3,4] In this regard, locomotion of micro/nanorobots represents a significant advantage compared to traditional systems.[5,6] For instance, previously inaccessible routes in the body can be utilized for active reach to target locations by utilizing various propulsion sources.[7–15] In addition to locomotion features, micro/nanorobots enable modification possibilities, *e.g.*, cargo loading, coating, and/or functionalization, depending on the intended application.[16–20]

[a]*Future Energy and Innovation Laboratory, Central European Institute of Technology, Brno University of Technology, Purkynova 123, 61200 Brno, Czech Republic. E-mail: martin.pumera@ceitec.vutbr.cz*
[b]*Faculty of Electrical Engineering and Computer Science, VSB – Technical University of Ostrava, 17. Listopadu 2172/15, 70800 Ostrava, Czech Republic*

**Cagatay M. Oral**

*Cagatay M. Oral is a Ph.D. student at Central European Institute of Technology (CEITEC), Brno, Czech Republic. He received his B.S. and M.S. degrees from Metallurgical and Materials Engineering Department at Middle East Technical University (METU), Ankara, Turkey. During his studies at METU, he focused on the synthesis of calcium-based particles for orthopedic applications. Currently, he is developing micro/nanorobots for biomedical and environmental applications.*

**Martin Pumera**

*Martin Pumera is the Director of the Center for Advanced Functional Nanorobots and a Distinguished Professor of Chemistry at the University of Chemistry and Technology, Prague, and Chief Investigator of Future Energy & Innovation Lab at CEITEC, Brno, Czech Republic. He received his Ph.D. in 2001 from Charles University, Czech Republic. He became a tenured group leader at National Institute for Materials Science (NIMS), Japan, in 2006 and joined Nanyang Technological University, Singapore, as a professor in 2010. He has interests in nanomaterials, 3D printing, electrochemistry, and micro/nanomachines. He has been "Highly Cited Researcher" by Clarivate Analytics since 2017.*

Published on 27 April 2023. Downloaded on 4/10/2026 3:20:11 AM.

In this review, biomedical applications of micro/nanorobots are discussed by focusing on the preclinical studies conducted with animal models. To this end, actuation methods of micro/nanorobots are introduced initially to reveal the potential sources of locomotion *in vivo*. Then, the preclinical studies are discussed based on the suggested application areas to provide a comprehensive overview of the current approaches utilized in organs and other body parts (Fig. 1). Lastly, key challenges and future directions are highlighted toward the translation of micro/nanorobots from bench to bedside.

## 2. Actuation of micro/nanorobots

As a challenging operating environment, the body can readily restrict the locomotion of micro/nanorobots with biological barriers, confined spaces, and non-Newtonian fluids.[21] Additionally, the scale of micro/nanorobots further leads to challenges since traditional power components are not convenient for incorporation in their structures, which indicates the requirement of effective strategies to harvest energy for propulsion. To overcome these obstacles, various actuation methods have been proposed (Table 1). In general, the sources of active propulsion can be classified into two categories: (i) on-board and (ii) off-board methods. For the micro/nanorobots actuated with an on-board method, the power source can be local (chemical reactions) or biological (motile microorganisms).[22–29] Chemical reactions were widely utilized as the locomotion source in the early studies conducted with animal models.[30] For instance, microrobots based on magnesium (Mg) and zinc (Zn) hold the ability to react with water- and/or acid-based biofluids.[25,31,32] Due to these reactions, Mg- and Zn-based microrobots can produce hydrogen ($H_2$) bubbles, leading to propulsion in the stomach and/or intestine.[33–37] An asymmetric platinum coating or deposition can also provide bubble-propelled motion upon contact with fuel, *i.e.*, hydrogen peroxide ($H_2O_2$).[38,39] Although it is a convenient approach to obtain self-propelled micro/nanorobots, the toxicity of $H_2O_2$ constrains practical biomedical applications. In contrast to Pt-based structures, enzymes can be exploited as a biocompatible alternative. With enzymes immobilized on the surface of particles, enzymatic conversion of fuels (urea, glucose, *etc.*) may produce sufficient force to propel micro/nanorobots *in vivo*.[40–44]

Biological swimmers also act as a potent source of propulsion for microrobots. In this on-board actuation approach, motile organisms, *e.g.*, algae,[34] sperm,[45] and bacteria,[46] are coupled with nonmotile objects to constitute biohybrid microrobots that can have inherent actuation capabilities, even in harsh environments.[47] Compared to synthetic microrobots, biohybrid counterparts can provide a higher level of autonomy by sensing the changes in the local environment and demonstrating active response.[48]

Off-board actuation methods significantly differ from on-board methods with the requirement of utilizing external power sources (magnetic fields, acoustic waves, and light irradiation) for propulsion.[49] Among these sources, magnetic actuation is the leading way to precisely manipulate micro/nanorobots with high degrees of freedom (DoF).[50,51] Given the high penetration ability of magnetic fields, this approach is

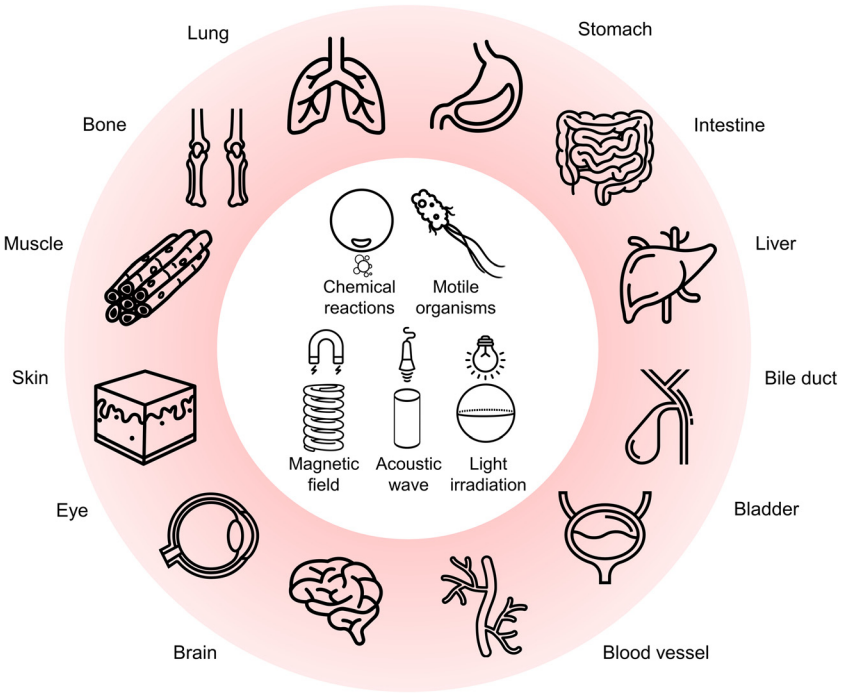


**Fig. 1** Target locations of the body treated with micro/nanorobots having different actuation methods.

 This journal is © The Royal Society of Chemistry 2023

Table 1 Overview of micro/nanorobots utilized for various treatments *in vivo*

| Micro/nanorobot structure | Active component | Motion source | Target location | Treatment | Approach | Ref. |
|---|---|---|---|---|---|---|
| $TiO_2$/PLGA/Fe-Se@chitosan-coated Mg microspheres | Mg | Chemical reactions | Intestine | Iron deficiency anemia | Mineral delivery | 71 |
| Mo–Pt–Pd-coated Janus carbon nanospheres | Mo–Pt–Pd | Chemical reactions | Brain | Traumatic brain injury | ROS scavenging | 72 |
| Nanoparticle-coupled microalgae (*C. reinhardtii*) | Microalgae | Self-propulsion | Lung | Pneumonia | Drug delivery | 73 |
| $Fe_3O_4$@PDA-coupled microalgae (*V. aureus*) | Microalgae/ $Fe_3O_4$ | Self-propulsion/ magnetic fields | Subcutaneous tissue | Tumor | Photodynamic and photothermal therapy | 74 |
| PDA/$Fe_3O_4$-coated microalgae (*S. platensis*) | $Fe_3O_4$ | Magnetic fields | Subcutaneous tissue | Bacterial infection | Photothermal therapy | 75 |
| $CaO_2$ nanoparticle-loaded Janus microrods | $CaO_2$ | Acoustic waves | Blood vessel | Thrombus | Sonodynamic therapy | 76 |
| Pt nanoparticle-containing silica nanospheres | Pt | NIR irradiation | Subcutaneous tissue | Tumor | Photothermal therapy and drug delivery | 77 |

Published on 27 April 2023. Downloaded on 4/10/2026 3:20:11 AM.

especially attractive for biomedical applications requiring precisely controlled motion in deep tissues.[52–59] Additionally, acoustic waves can produce robust propulsion even in dynamic fluids by generating resonance or complex acoustic patterns.[3,21,60] Similar to magnetic fields, acoustic waves are appealing for applications in deep tissues while minimally affecting the surrounding environment.[61–64] The use of light may also be considered as an effective stimulus for powering micro/nanorobots.[12,65] On the other hand, ultraviolet (UV) light can cause severe side effects, while visible (Vis) light has poor penetration depth into the tissue.[66,67] In general, near-infrared (NIR) light can provide both safety and considerable penetration depth to enable the configurable locomotion of micro/nanorobots *in vivo*.[68–70]

## 3. Digestive system

Oral and intravenous routes are the most common ways for micro/nanorobot administration to the body. The former was widely preferred in the early studies on artificial microrobots since it enables straightforward access to several organs in the digestive system, such as the stomach and intestine.

### 3.1. Stomach

In 2015, Wang and co-workers utilized bilayer poly(3,4-ethylenedioxythiophene)/Zn (PEDOT/Zn) microrobots for the delivery of gold (Au) nanoparticles to the stomach tissue.[78] The microrobots demonstrated gradual dissolution in the gastric acid due to the presence of Zn, leading to self-propulsion by generating $H_2$ bubbles (Fig. 2a). Furthermore, this self-destruction property enabled autonomous cargo delivery *in vivo* without leaving anything toxic behind. In another study, the same research group presented tubular microrobots having two different compartments (Zn-based propellant engine and cargo-loaded gelatin segment), as shown in Fig. 2b.[79] The microrobots displayed a tunable lifetime during their self-propulsion in the gastric acid depending on the Zn engine's length. Additionally, a pH-responsive cap protected the cargo-loaded gelatin segment. Once the microrobots penetrated the gastric mucosa (pH $\geq$ 6), the pH-responsive cap dissolved and promoted a localized cargo release to the stomach wall.

In addition to Zn-based microrobots, the stomach's acidic environment enabled the use of Mg as the active component for microrobot locomotion. For instance, self-propelled Mg-based microrobots were investigated to treat *H. pylori* infection as a model disease.[80] To obtain an antibacterial drug delivery platform, spherical Mg particles were successively coated with titanium dioxide ($TiO_2$), antibiotic-loaded poly(lactic-*co*-glycolic acid) (PLGA), and chitosan layers while keeping a small part of the surface uncoated. With this asymmetric coating approach, the release of $H_2$ bubbles could lead to an efficient self-propulsion upon contact with gastric acid (Fig. 2c). Thanks to the active motion in a mouse stomach model, the microrobots could effectively deliver the antibiotic (clarithromycin), which could significantly reduce the bacterial burden compared to the condition involving drug-loaded passive particles.

To deliver payloads in the stomach, oral administration of microrobot suspensions is a straightforward way. However, existing robotic systems are prone to have limited applicability *in vivo* due to short propulsion times in body fluids. Related to this limitation, the utilization of pills was proposed to overcome microrobots' premature loss before reaching target locations.[81] The pills consisted of Mg/$TiO_2$/PLGA microrobots uniformly dispersed in the matrix having inactive excipients (lactose and maltose) and disintegration-aiding additives (cellulose and starch). When the pills encountered the acidic stomach environment, the sugar matrix dissolved quickly to release the microrobots (Fig. 2d). Afterward, the microrobots could demonstrate locomotion in the gastric fluid by generating $H_2$ bubbles owing to the Mg cores. *In vivo* gastric retention studies showed that microrobot-containing pills could provide a more concentrated release of the microrobots compared to the control groups where the microrobots were administered in a solution or with pills containing nonmotile particles. With these results, microrobot-containing pills indicated a promising way of carrying microrobots with utmost protection to facilitate delivery at targeted locations.

Published on 27 April 2023. Downloaded on 4/10/2026 3:20:11 AM.

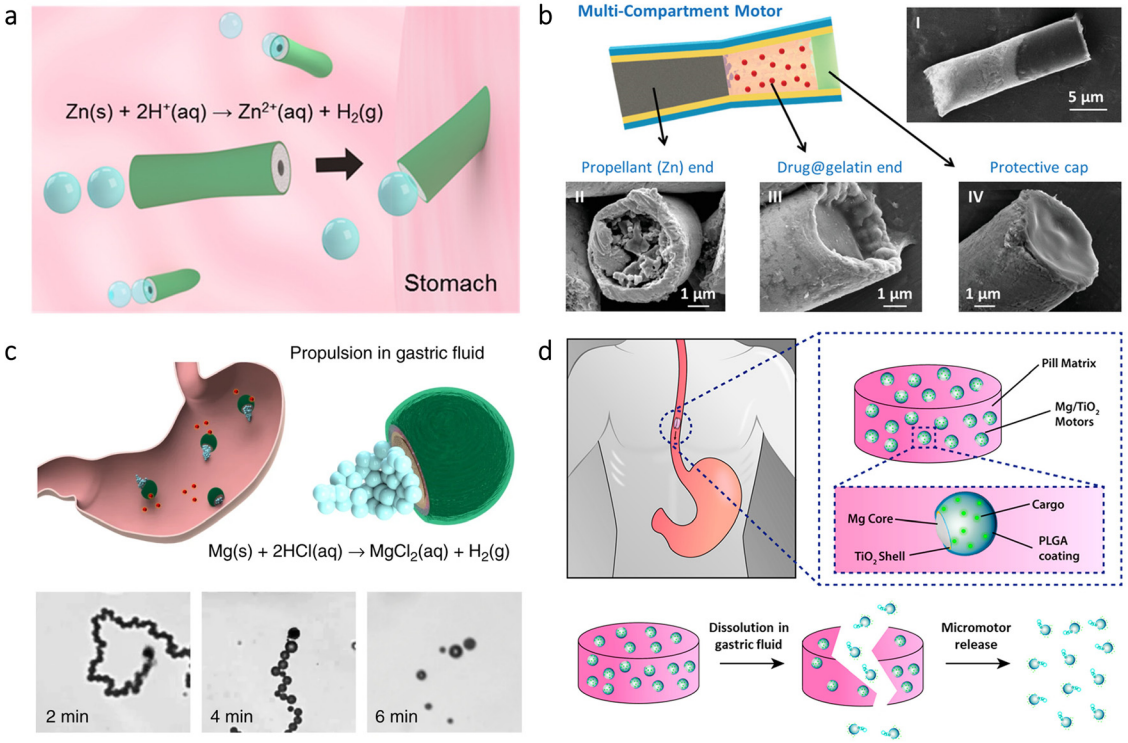


**Fig. 2** Bubble-propelled microrobots in the stomach. (a) Zn-based tubular microrobots for tissue penetration *in vivo*. Reproduced with permission.[78] Copyright 2015, American Chemical Society. (b) SEM images of (I) tubular multicompartment microrobots having (II) Zn-based propellant compartment, (III) cargo-loaded gelatin compartment, and (IV) protective enteric cap. Reproduced with permission.[79] Copyright 2020, Wiley-VCH. (c) Motion mechanism of Mg-based microrobots in a mouse stomach. Images show bubble-propelled propulsion of the microrobots in the gastric fluid. Reproduced with permission.[80] Copyright 2017, Springer Nature. (d) Disk-shaped pills and their dissolution in the gastric fluid to release the encapsulated microrobots. Reproduced with permission.[81] Copyright 2018, American Chemical Society.

### 3.2. Intestine

Micro/nanorobots administered *via* the oral route can reach the intestine from the stomach; however, proper measures may be needed on their structures to preserve an inactive stage in the stomach. For instance, to precisely position the microrobots for site-specific delivery applications, an enteric polymer coating was utilized on PEDOT/Au microrobots loaded with Mg microspheres.[82] This coating shielded the microrobots from the acidic gastric fluid (pH 1–3), whereas it enabled dissolution in the intestinal fluid (pH 6–7) to initiate the self-propelled microrobot motion in the intestine (Fig. 3a). Additionally, tunable thickness of the pH-sensitive enteric polymer coating led to selective activation of the microrobots in desired regions of the intestine. With this way, the microrobots demonstrated promising results to enable localized tissue penetration and enhanced retention.

In another study, Mg-based microrobots were proposed for the treatment of anemia.[71] Thanks to the self-propulsion of microrobots in gastrointestinal (GI) fluid, active delivery of iron (Fe) and selenium (Se) was obtained in the intestine. *In vivo* experiments showed that the hematological parameters of an anemic mouse could be normalized after 30 days of treatment with the microrobots, while showing no toxic effect. An oral vaccination platform was also obtained using Mg-based microrobots.[83] Upon delivery *via* the oral route, microrobots' self-propulsion could significantly improve retention and uptake of the antigens in the intestine, leading to a significantly higher generation of antibody titers compared to the conditions involving nonmotile particles.

Light irradiation has also been utilized in the intestine toward different purposes. For instance, microrobot-containing microcapsules were designed to have disintegration ability on demand upon NIR irradiation.[84] Since this platform was imaged with photoacoustic computed tomography (PACT) in real-time, self-propelled Mg-based microrobots could be released from the microcapsules precisely at target locations to deliver drugs (Fig. 3b). Another type of application was treating colorectal cancer *via* NIR light-driven nanorobots.[85] The nanorobots consisted of Pt-coated mesoporous silica having a specific camouflage (*S. aureus* membrane) and a chemotherapeutic drug (cisplatin). While NIR light provided the stimulus for the motion, the biomimetic camouflage guided the nanorobots toward the intestinal site of colorectal cancer, as demonstrated in Fig. 3c. This chemotactic property provided 4.3-fold higher anchoring at the tumor site compared to the nanorobots lacking this property. Considering also 14.6-fold higher penetration to mucus, a significant tumor inhibition rate

 This journal is © The Royal Society of Chemistry 2023

Published on 27 April 2023. Downloaded on 4/10/2026 3:20:11 AM.

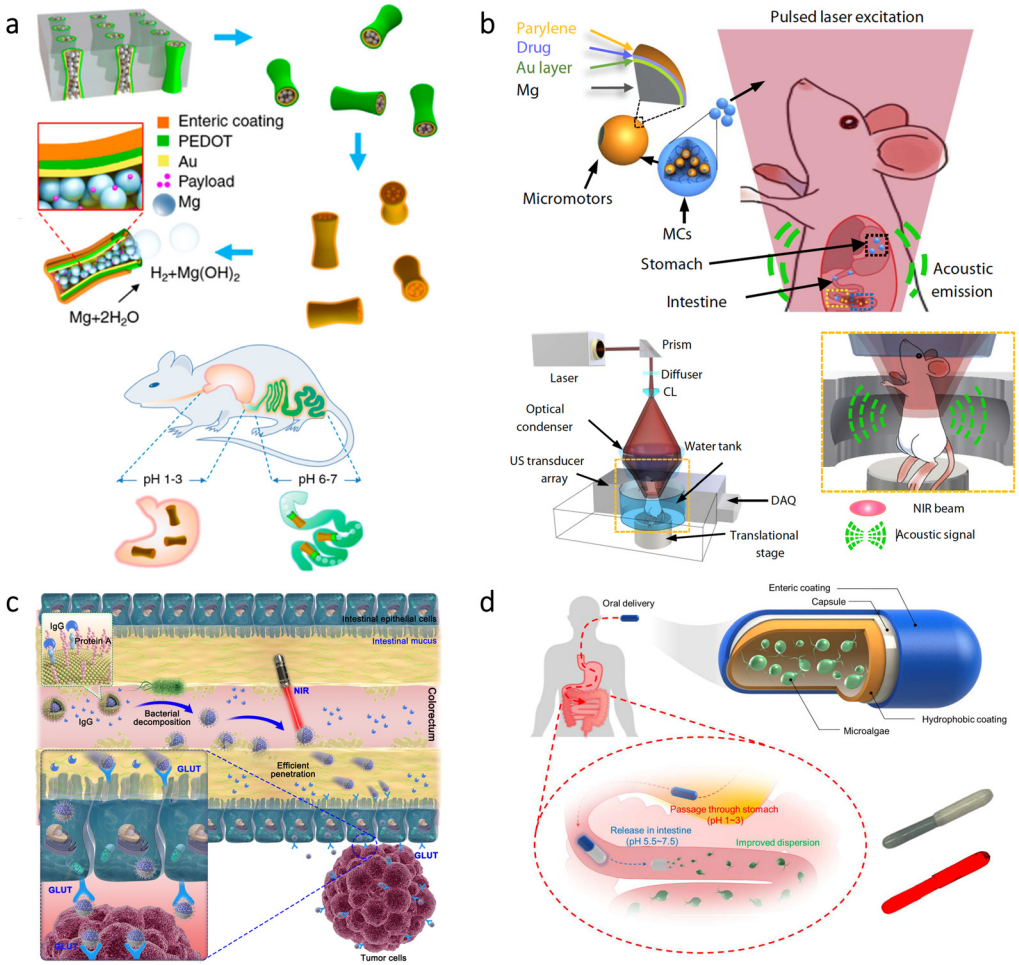


**Fig. 3** Micro/nanorobots in the intestine. (a) Preparation of PEDOT/Au microrobots *via* an electrodeposition method and their coating with an enteric polymer. Schematic illustration of the mouse demonstrates localized microrobot propulsion upon pH-sensitive dissolution of the enteric coating. Adapted with permission.[82] Copyright 2016, American Chemical Society. (b) Microrobot-containing capsules having disintegration ability with NIR light irradiation and their real-time imaging principle *via* PACT. Reproduced with permission.[84] Copyright 2019, American Association for the Advancement of Science. (c) NIR light-driven nanorobots with mucus penetration ability to deliver a chemotherapeutic drug for the treatment of colorectal cancer. Reproduced with permission.[85] Copyright 2022, American Association for the Advancement of Science. (d) Protective capsules loaded with algae-based microrobots as self-motile drug delivery platforms. The inset shows bright-field (top) and fluorescent (bottom) images of algae-loaded capsules. Adapted with permission.[86] Copyright 2022, American Association for the Advancement of Science.

(99.1%) was observed with the help of NIR light-driven nanorobots.

More recently, self-motile microorganisms were investigated for enhancing cargo delivery in the intestine.[86] Toward this purpose, a microalgae species (*C. reinhardtii*) was functionalized with drug-containing polymeric nanoparticles, and then they were embedded inside a protective capsule for safe passage through the stomach's harsh acidic environment (Fig. 3d). Upon release from the capsule, algae could display long-lasting swimming behavior significantly higher than Mg-based microrobots. The results of *in vivo* experiments demonstrated that intestinal distribution and drug retention could improve thanks to the prolonged motility of the microrobots, which highlights the potential of motile microorganisms as autonomous cargo carriers *in vivo*.

### 3.3. Liver

The liver may contain solid tumors that are challenging to penetrate due to the high interstitial fluid pressure.[87] As a promising approach, magnetic microrobots were proposed to deliver drugs/cells into tumors with their robust locomotion strategies.[88,89] For example, mesenchymal stem cells were delivered to the liver using microrobots under the guidance of photoacoustic (PA) imaging.[54] The microrobots were designed to be burr-like porous spheres with a structure consisting of poly(ethylene glycol) diacrylate and pentaerythritol triacrylate to ensure mechanical stability and degradability concurrently. Additionally, $Fe_3O_4$ nanoparticles were incorporated into the structure for magnetic navigability during PA imaging of the microrobots *in vivo*. In this study, the delivery experiments

Published on 27 April 2023. Downloaded on 4/10/2026 3:20:11 AM.

were performed using mice having orthotopic liver tumors. The results showed that tumor growth could be inhibited with the successful delivery of the stem cells and their migration into the tumor tissue.

In addition to the treatments for solid tumors, microrobots were used for hemorrhage treatment in the liver.[90] For this application, self-propelled starch-based Janus microrobots were used because of the microporous starch's ability to lead hemostasis by concentrating blood coagulation factors with its sieve-like porosity.[91] Additionally, calcium carbonate ($CaCO_3$) was grown on the other half of the Janus structure as the engine producing strong bubbles against blood flow, which can facilitate the reach to the deep bleeding sites. In the experiments conducted using liver bleeding models, standard gauze was found inadequate for controlling the bleeding, whereas the self-propelled microrobots successfully halted the bleeding in the minimum time (48 ± 5 s). This effective treatment also led to the lowest blood loss for rabbits, resulting in the highest survival rate after surgery (100%).

### 3.4. Bile duct

The bile duct consists of thin tubes that carry bile from the liver and gallbladder to the small intestine. In an early attempt to investigate microrobots through *in vivo* experiments, microgrippers were used as autonomous robotic tools to collect tissue samples in this hard-to-reach body part.[92] The microgrippers had a star-like shape, consisting of a thermo-sensitive polymeric trigger and multicomponent layers. Their responsive design could enable modification of this shape upon exposure to the body temperature, while nickel's presence led collectability of the microgrippers with an applied magnetic field. In a porcine model, the microgrippers were injected into the biliary orifice and retrieved after 10 min using a magnetic catheter. Then, these microgrippers were investigated in terms of the tissue they collected. Further analysis showed that the tissue samples were sufficient to allow the identification of genetic markers for various diseases, indicating the possibility of precise diagnostics in hard-to-reach areas of the body *via* autonomous microrobots.

## 4. Urinary system

The urinary system is responsible for filtering blood to remove toxins and waste through urine, which contains urea as a potent fuel for micro/nanorobot motion. This section covers the studies conducted with bladder models for cancer therapy and imaging applications.

### 4.1. Bladder

Bladder cancer is the 9$^{th}$ most common cancer globally, and it has a substantial recurrence rate (≈50%).[93] Although intravesical chemotherapy can be utilized as a standard treatment for bladder cancer, urination significantly decreases drug residence time in the bladder.[93,94] Therefore, to enhance efficacy of treatments, high penetrability into cancerous sites is highly required. In a recent study, a microrobotic approach was developed using cells as active "Trojan horse" for the sustainable delivery of adenovirus (a type of oncolytic virus for cancer virotherapy) as shown in Fig. 4a.[95] The microrobots were based on human embryonic kidney cells (293T) modified with cyclic arginine–glycine–aspartic acid tripeptide (cRGD) to ensure specific binding with bladder cancer cells. Besides, asymmetrically immobilized $Fe_3O_4$ nanoparticles on the surface of 293T cells led to microrobot motion *via* external rotating magnetic fields. According to the results of experiments conducted with tumor-bearing mice, magnetic control led to a 4.6-fold decrease in bioluminescence intensity as an indicator of bladder tumor growth. This effective decrease was associated with prolonged retention and improved tissue penetration realized by the robust microrobot motion *via* external magnetic fields. Additionally, the observation of tumor inhibition was supported by an analysis of the overall survival rate, where mouse death occurred in all groups except the condition having the microrobots under magnetic control.

The bladder has also been a model organ to investigate imaging modalities for microrobots' real-time tracking in the body. As an example, PA imaging was recently combined with high-frequency ultrasound (HFUS) to obtain molecular and anatomical feedback from the mouse bladder.[96] This dual imaging technique demonstrated competence to provide real-time images with its ability to discriminate endogenous signals from motile microrobots. In another study, positron emission tomography (PET) was combined with computed tomography (CT) to track the swarm behavior of self-propelled nanorobots.[97] The nanorobots were based on mesoporous silica nanoparticles having urease enzyme and gold nanoparticles at their surfaces (Fig. 4b). The presence of urease enzyme enabled decomposition of the fuel (urea) into carbon dioxide and ammonia, resulting in a self-propelled motion. Additionally, the nanorobots were radiolabeled with iodine-124 or fluorine-18 isotopes for imaging purposes. This multifunctional design allowed tracking of nanorobot motion in the mouse bladder. Together with the imaging possibility, this study indicated that swarming behavior of the nanorobots could be beneficial for drug delivery purposes toward the treatment of bladder diseases.

## 5. Nervous system

The nervous system controls various aspects of body functions. Since it enables communication and coordination between the systems, any disease in the nervous system can pose a serious threat to the body. In this section, micro/nanorobotic treatments are explicitly discussed for the brain.

### 5.1. Brain

The blood–brain barrier (BBB) represents a significant challenge for treatments in the brain due to its ability to block foreign substances' entry from blood.[98,99] As a noteworthy approach to cross the BBB, researchers utilized a natural

 This journal is © The Royal Society of Chemistry 2023

Published on 27 April 2023. Downloaded on 4/10/2026 3:20:11 AM.

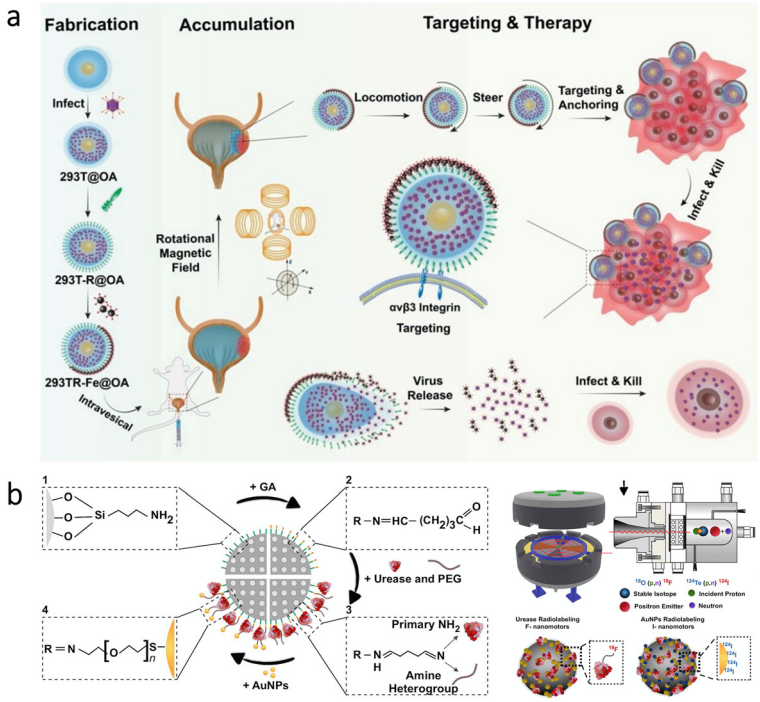


**Fig. 4** Micro/nanorobots in the bladder. (a) Preparation of virus-loaded cell-based magnetic microrobots having targeting capabilities for bladder cancer cells. After the release of virus from the microrobots, oncolytic virotherapy can be obtained by infection of the surrounding tumor site. Reproduced with permission.[95] Copyright 2022, Wiley-VCH (b) Urease and gold-functionalized silica nanorobots and their radiolabeling for *in vivo* imaging applications. Adapted with permission.[97] Copyright 2021, American Association for the Advancement of Science.

phenomenon, the high flow of glucose from blood to the brain. To this end, nanometer-sized polymersomes (vesicles formed by the self-assembly of amphiphilic copolymers) were prepared with chemotaxis behavior (directed motion toward or away from specific chemicals) in the presence of a glucose gradient (Fig. 5a).[100] The nanorobot motion was obtained with D-glucono-δ-lactone and $H_2O_2$ formed by the encapsulated glucose oxidase, while encapsulated catalase decomposed $H_2O_2$ to enhance the chemotactic behavior further. As a significant advantage, using these enzymes in tandem led to locomotion without releasing gaseous oxygen and $H_2O_2$. Moreover, *in vivo* experiments demonstrated that a 4-fold increase in penetration to the brain could be achieved using chemotactic nanorobots having protein targeting compared to non-active polymersomes.

As a disease impacting the brain significantly, acute ischemic stroke may cause permanent damage and dysfunction by blocking blood flow. Recent studies reported that the pathogenesis of ischemic stroke could be related to the excessive production of reactive oxygen species (ROS) and the up-regulation of inflammatory factors. Since $H_2$ therapy can scavenge ROS and down-regulate inflammatory factors, researchers investigated asymmetrically coated Mg microrobots in the middle cerebral artery (MCA) occlusion of rats.[24] With their considerable speed (51.1 μm $s^{-1}$ in artificial cerebrospinal fluid), the microrobots enhanced the permeation of $H_2$ into the deep brain tissue, which led to a significant decrease in infarct volume and improved spatial learning capacity. As an additional advantage, the utilization of PLGA-coated Mg particles allowed gradual depletion with complete disappearance ability after the therapy.

For the treatment of neurological disorders, *e.g.*, brain tumors, Alzheimer's disease, and Parkinson's disease, stem cells can provide an efficient therapeutic effect thanks to their ability to differentiate a variety of cell types. However, their delivery to specific parts of the brain is a significant challenge while having minimal invasion. To overcome this challenge, stem cell-based magnetic microrobots were developed.[101] Stem cells were collected from the nasal turbinate tissue of patients, and they were magnetized by the internalization of superparamagnetic iron oxide nanoparticles (SPIONs). Then, these microrobots were administered to a mouse *via* the intranasal pathway to bypass the BBB. The results of *in vivo* experiments showed that the microrobots could be guided to the target area in brain tissue under the influence of a magnetic field, whereas the microrobots remained near the olfactory bulb when there was no applied magnetic field. Although these results are promising, for such targeted delivery applications, real-time imaging plays an essential role in enhancing the performance of externally driven microrobots. Recently, optoacoustic tomography (OAT) was proposed for real-time detection and tracking of microrobots circulating in the brain vasculature.[102] As shown in Fig. 5b, researchers prepared silica microrobots having nickel (Ni) coating to enable magnetic manipu-

Published on 27 April 2023. Downloaded on 4/10/2026 3:20:11 AM.

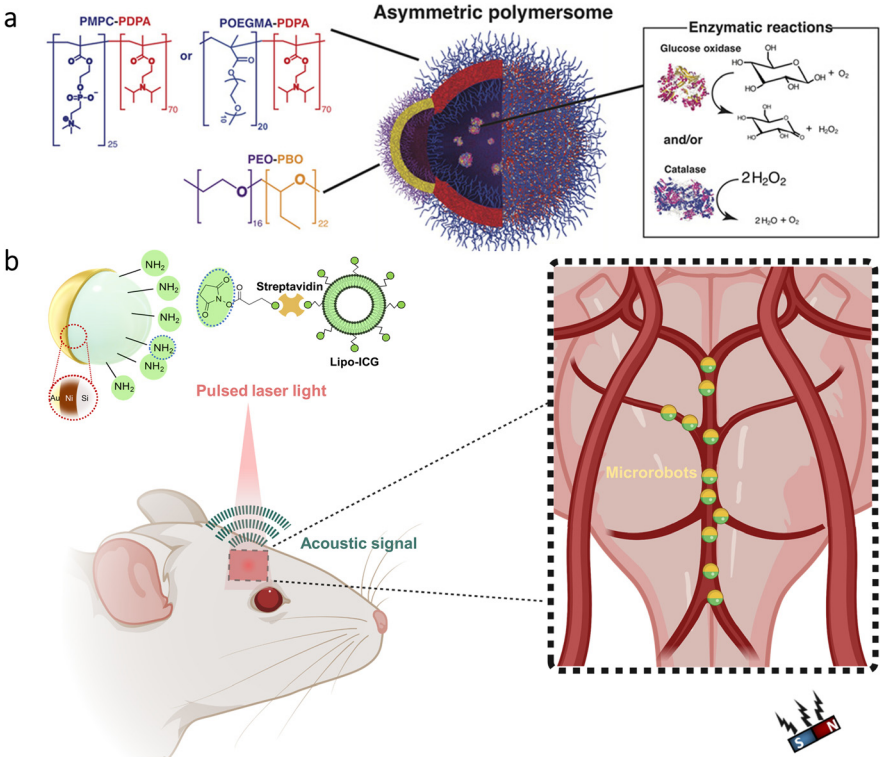


**Fig. 5** Micro/nanorobots in the brain. (a) Enzyme-containing asymmetric polymersomes with chemotaxis behavior for crossing the BBB. Reproduced with permission.[100] Copyright 2017, American Association for the Advancement of Science. (b) Schematic of magnetic microrobots having Au and liposome ICG coatings for OAT of the microrobots inside the mouse brain vasculature. The magnet indicates the microrobots' manipulation capability *in vivo*. Adapted with permission.[102] Copyright 2022, American Association for the Advancement of Science.

lation *in vivo*. Additionally, the microrobots were designed to have ICG-entrapped nanoliposome and Au coatings to enhance the OAT contrast. Thanks to the specific design, these microrobots could be tracked with three-dimensional (3D) real-time images in the circle of Willis. Manipulation of the microrobots was also demonstrated inside the brain vasculature with a permanent magnet, which indicates their potential use for site-specific applications in intravascular environments.

## 6. Cardiovascular system

As part of the cardiovascular system, blood vessels supply oxygen and nutrients throughout the body. Due to the significance of this task for healthy tissue, obstructions in the blood vessels require targeted and delicate treatments. In other respects, controlled blocking of the blood flow can also be part of site-specific treatments, such as tumor therapy. In this section, micro/nanorobotic strategies are discussed for restoring or blocking blood flow.

### 6.1. Blood vessels

Among cardiovascular diseases, obstruction of blood vessels is a widespread health problem with the possibility of causing catastrophic events, such as stroke, infarction, and embolism.[76,103–106] The Food and Drug Administration (FDA) approved the use of tissue plasminogen activator (tPA) as a potential approach to attain rapid thrombus clearance. However, the short time window for therapy and toxic side effects at high application doses represent the main challenges of this approach. As a noteworthy way of enhancing the delivery of tPA at target sites, researchers used a swarm of $Fe_3O_4$ nanorobots.[107] For *in vivo* experiments, they also developed a C-shaped magnetic system and combined it with an ultrasound imaging device to monitor the nanorobots (Fig. 6a). Guiding tPA toward thrombus with the help of magnetic swarm led to rapid recanalization at the embolic site of a rabbit model. On the contrary, drug treatment without the swarm provided only a stepwise dissolution of the thrombus. The measurements demonstrated that the combined treatment could decrease the thrombus area by ≈53.5%, whereas this value was ≈10.0% for drug treatment alone.

Other approaches were also proposed for thrombolysis using distinct micro/nanorobots. For example, inspired by a natural phenomenon -endothelial cells' nitric oxide (NO) production to prevent thrombosis-, researchers presented light-driven nanorobots that can produce NO gas bubbles.[108] In this way, they aimed mechanical and photothermal treatment by deep penetration into the thrombus (Fig. 6b). The nanorobots

 This journal is © The Royal Society of Chemistry 2023

Published on 27 April 2023. Downloaded on 4/10/2026 3:20:11 AM.

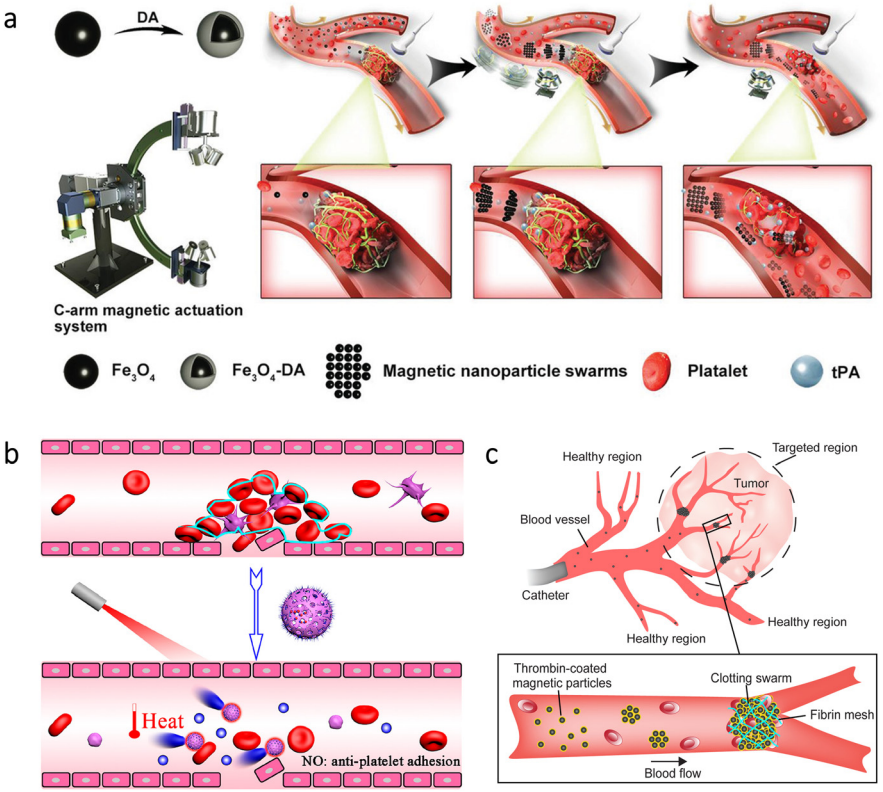


**Fig. 6** Recanalization or blockage of blood vessels *via* micro/nanorobots. (a) Manipulation of magnetic swarms under a C-shaped actuation system and an ultrasound imaging device to enhance the drug delivery for thrombolysis. Reproduced with permission.[107] Copyright 2021, Wiley-VCH. (b) NIR light-driven nanorobots for mechanical and photothermal thrombus treatment. Reproduced with permission.[108] Copyright 2021, American Chemical Society. (c) Thrombin-coated magnetic microrobots to lead swarms that can block the blood flow in target regions, *e.g.*, tumor environments. Reproduced with permission.[110] Copyright 2022, American Association for the Advancement of Science.

consisted of hollow polydopamine (PDA) particles modified with Cys-Arg-Glu-Lys-Ala (CREKA) peptide. Additionally, a donor for NO was loaded to these nanorobots, leading to an efficient bubble-driven motion under NIR light irradiation. After observing the motion behavior, the nanorobots were further evaluated with mice having thrombus in their tails. According to the histological analysis, there was no clear indication of blood clots for the group treated with nanorobots and NIR light irradiation. As a noteworthy observation, this treatment also prevented the reoccurrence of thrombus *in vivo*. In another study, a combined treatment for atherosclerosis was proposed to prevent its severe consequences in the body.[109] This treatment involved a balloon having a coating of drug-loaded NIR-driven nanorobots. Initially, $Fe_3O_4$ nanoparticles were used as sacrificial templates to obtain mesoporous silica nanoparticles, and then Pt was sputtered on one side of the nanorobots. Anti-proliferative paclitaxel (PTX) drug and anti-vascular cell adhesion molecule-1 (anti-VCAM-1) targeting antibody were additionally incorporated into the structure, and platelet membrane was used as a coating. In the carotid artery of rabbits, the combined effect of drug-loaded nanorobots and photothermal therapy led to a significantly lower plaque area.

For the studies discussed above, the main concept was to utilize micro/nanorobots to maintain the flow in blood vessels. In a more recent study, the opposite of this approach -blocking the blood flow- was proposed *via* magnetic swarms as a potential treatment for tumors and arteriovenous malformations.[110] The swarm consisted of magnetic particles coated with thrombin due to its ability to convert soluble fibrinogen into fibrin meshes. With this way, the trapping of red blood cells was aimed to form a clotting swarm that could block the blood flow, as demonstrated in Fig. 6c. This approach was tested in the blood vessels of porcine kidneys *in vivo*. When selected areas were exposed to dynamic magnetic fields for 10 min, embolization was successfully obtained only in these areas. Although obstructions in blood vessels are mostly harmful to the body, this study successfully demonstrated that they could also be part of an effective tumor treatment thanks to the precise control of magnetic microrobots.

## 7. Other systems

Micro/nanorobots have also been utilized in challenging locations of the body in terms of locomotion. In this section,

Published on 27 April 2023. Downloaded on 4/10/2026 3:20:11 AM.

micro/nanorobotic treatments are summarized for complications related to the eye, skin, muscle, bone, and lung.

### 7.1. Eye

The eye is mainly divided into anterior (front) and posterior (back) segments. For the treatment of ocular diseases, drugs can be administered *via* eye drops or operations can be performed surgically. However, these treatments may be insufficient for the diseases in the posterior segment, highlighting the need for active systems to access all eye segments.[66,111] Magnetic microrobots hold great promise within this context thanks to their robust motion and external controllability.[112–114] For instance, cylindrical magnetic microrobots were tested in the eye of rabbits for minimally invasive intraocular surgery.[115] Despite the challenges of the operating environment (viscoelasticity of the vitreous and the presence of collagen fiber bundles), the microrobots could be steered in the eye with an electromagnetic control system. When the microsurgery is completed, they could also enable removal from the vitreous cavity by a magnetic tool. Upon further development in the design, such magnetic microrobots can hold significant potential for future applications in the eye requiring localized mechanical manipulations or targeted drug delivery with minimal invasion.

### 7.2. Skin

In the microrobotics field, an early study aimed infrared laser-assisted tissue welding *in vivo*.[116] The microrobots consisted of silica particles having polyelectrolyte multilayers and $Fe_3O_4$ nanoparticles. One side of the microrobots was also coated with Au to create a Janus structure. Then, the microrobots were inserted into deep cuts on the mouse skin, followed by the wound's closure with a laser. Thanks to thermophoretic motion and magnetic attraction abilities, the microrobots could provide a sealing effect for bleeding wounds *in vivo*.

More recently, self-propelled nanorobots were utilized to treat diabetic foot ulcers.[117] For this application, researchers prepared calcium peroxide ($CaO_2$) nanoparticles capped with PDA layers. The nanorobots could release NO due to their specific surface design with the aim of eliminating bacterial infections in the skin wounds of diabetic mice. Enzyme-powered microrobots were also used to treat abscess infections.[118] In order to obtain self-propelled microrobot motion in the presence of fuel (urea), urease enzyme was attached to silica particles. Additionally, the microrobots were functionalized with a cationic antimicrobial peptide (LL-37), which can lyse bacterial cells by disrupting the membranes. After inducing skin infection with a Gram-negative bacterial strain (*A. baumannii*), the microrobots and a urea solution were applied to the infected area (Fig. 7a). While free peptides could lead to only a localized effect around the initial administration site, the microrobots reduced the bacterial load by two orders of magnitude, indicating efficacy of the self-propelled microrobotic treatment.

Apart from the studies conducted on animal skin, subcutaneous tumor models have been a widely preferred way of investigating micro/nanorobots *in vivo*.[119–127] In general, different cancer cell lines, *e.g.*, breast and cervical, were subcutaneously injected into animals to establish tumors. When the tumor models reached a considerable size, micro/nanorobots were injected into the blood or directly into the tumor site. This approach enables the investigation of various robotic treatments through real-world conditions; however, more studies are required to analyze the locomotion performance of micro/nanorobots when the tumors are located in other parts of the body.

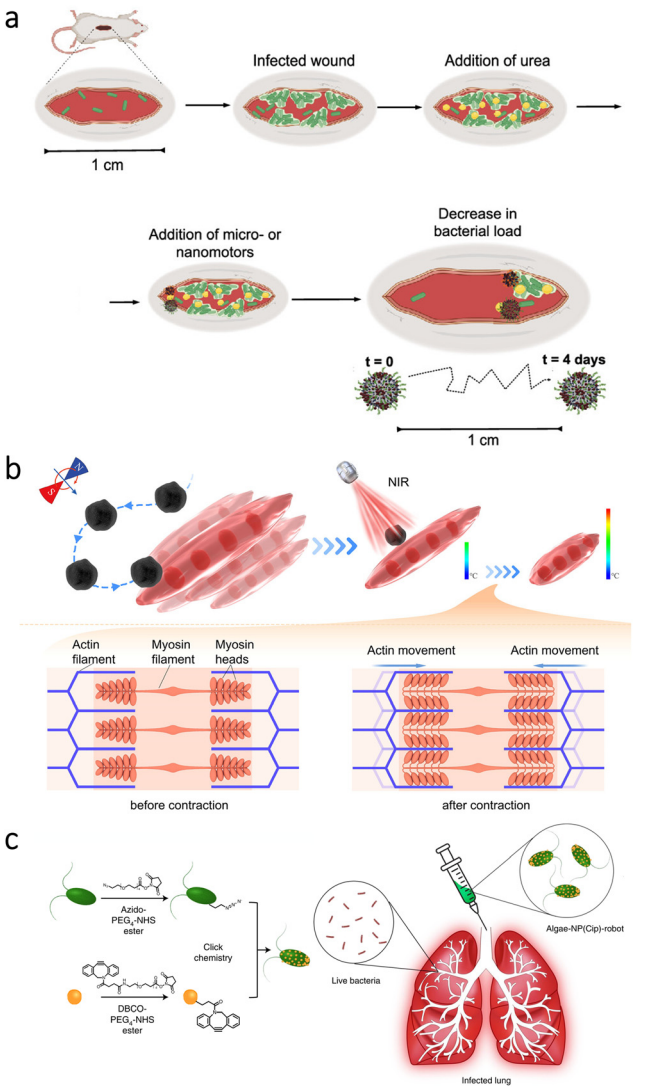


**Fig. 7** Microrobots for the treatment of skin-, muscle-, and lung-related complications. (a) Enzyme-powered antimicrobial microrobots toward the treatment of bacterial infections on the skin. Adapted with permission.[118] Copyright 2022, American Chemical Society. (b) Magnetic microrobots for targeted heat stimulus of myotubes under NIR light irradiation. Reproduced with permission.[128] Copyright 2022, American Chemical Society. (c) Functionalization of algae with drug-loaded nanoparticles using click chemistry and their intratracheal administration for the treatment of lung infections. Adapted with permission.[73] Copyright 2022, Springer Nature.


This journal is © The Royal Society of Chemistry 2023

Published on 27 April 2023. Downloaded on 4/10/2026 3:20:11 AM.

### 7.3. Muscle

Stimulation of muscle contraction has been considered as a practical approach to maintain muscle quality. On the other hand, most of the current strategies lack positioning capability for photothermal stimulation of specific locations. To overcome this limitation, researchers proposed the use of magnetic microrobots.[128] The microrobots were prepared by dip-coating a microalgae species (*C. pyrenoidosa*) with $Fe_3O_4$ nanoparticles. In addition to enabling magnetic navigability under the guidance of rotating magnetic fields, $Fe_3O_4$ nanoparticles could increase the local temperature upon NIR irradiation. By this temperature change, contraction in myotubes could be aimed (Fig. 7b). When manipulation capabilities of the microrobots were observed in the exposed muscle of a rat's leg, NIR light stimulus was applied to analyze contraction frequency of the muscle fibers. According to the results, the microrobots' presence led to a significant increase in intracellular temperature (from 0.8 ± 0.3 °C to 4.9 ± 0.6 °C), inducing a higher contraction frequency that can be beneficial for repairment without causing damage to the surrounding tissue. Although microrobot locomotion can be readily restricted in muscle tissue, this study presented a noteworthy application area for microrobots requiring further investigation.

### 7.4. Bone

The concept of utilizing Mg-based microrobots for ROS scavenging was also investigated to treat inflammation-related diseases in bone tissue. An example of such diseases is rheumatoid arthritis, an autoimmune disorder causing lifelong suffering and pain. Since active $H_2$ delivery can lead to ROS scavenging and down-regulation of inflammatory cytokines, PLGA- and hyaluronic acid-coated Mg microrobots were developed to treat this autoimmune disorder.[129] The sustained generation of $H_2$ bubbles could provide another advantage by enabling precise *in vivo* positioning of the microrobots under ultrasound guidance. For a rat model having collagen-induced arthritis, the use of Mg-based microrobots led to the slowest disease progression compared to the cases having Mg particles with passive $H_2$ release or a commercial anti-inflammatory drug (dexamethasone). Later, ROS scavenging was realized using $Fe_3O_4$ nanorobots that can be manipulated as swarms with a magnetic control system.[130] This swarming behavior eased real-time ultrasound imaging, allowing accurate targeting and positioning of the nanorobots to treat osteoarthritis. The experiments conducted in the knee joints of rats showed that magnetically controlled nanorobots could significantly suppress ROS expression more than their static counterparts.

Moreover, magnetic microrobots were used to deliver human adipose-derived mesenchymal stem cells for knee cartilage regeneration.[131] To this end, spherical PLGA microscaffolds were combined with magnetic microclusters consisting of ferumoxytol and chitosan. Afterward, the cells were loaded by seeding into each microrobot and incubating for 24 h. This loading caused only a 4.4% decrease in the average speed of the microrobots in the motion experiments conducted under a constant magnetic field (30 mT) and gradient (0.6 T $m^{-1}$). This study further explored the possibility of wearing a permanent magnet as a fixation tool after positioning the microrobots at the damaged cartilage. All these concepts were combined in a defect model of rabbit knee cartilage, where the results demonstrated an enhanced cartilage regeneration. Furthermore, the microrobots' design provided degradability in approximately 3 weeks under *in vivo* conditions without inflammation reactions or causing damage to the tissue.

### 7.5. Lung

In a recent study, biohybrid microrobots were proposed for the treatment of acute bacterial infections in the lungs.[73] For this treatment, a microalgae species (*C. reinhardtii*) was modified with neutrophil membrane-coated polymeric nanoparticles having antibiotic loading (ciprofloxacin). After establishing the drug-loaded self-motile platform (Fig. 7c), mice were intratracheally inoculated with *P. aeruginosa*, and then efficacy of the microrobotic treatment was analyzed. The results demonstrated that bacterial burden could be reduced up to three orders of magnitude thanks to biohybrid microrobots' active drug delivery performance. As an important observation, the mice treated with the microrobots resulted in 100% survival rate during the 14-day study, while all the untreated mice died in 3 days. These findings indicated biohybrid microrobots' superior drug delivery performance without requiring external guidance or specific fuel. With further development, such biohybrid platforms can pave the way for various treatments with a higher degree of autonomy *in vivo.*

## 8. Key challenges and future directions

The studies discussed in this review have demonstrated promising results for a variety of applications under *in vivo* conditions. However, considering the infancy of micro/nanorobotic treatments, there are still challenges to overcome. In this section, we discuss the challenges and potential remedies for the successful translation of micro/nanorobots from bench to bedside.

### 8.1. Safety

Ensuring safety is of utmost importance for micro/nanorobots in the biomedical field. To not cause any side effects in the short- and long-term, micro/nanorobots must be assessed in accordance with comprehensive regulations. At the initial stages of safety evaluation, the design and fabrication of micro/nanorobots should be considered. According to the international standard for "biological evaluation of medical devices (ISO 10993-1)", all components of a device are required to be biocompatible.[132] However, toxic materials have been used for various purposes in the micro/nanorobotic field. Nickel- and cobalt-based coatings are examples of such materials preferred due to their magnetic properties.[133]

Published on 27 April 2023. Downloaded on 4/10/2026 3:20:11 AM.

Instead, alternative materials, such as FePt coatings or $Fe_3O_4$ nanoparticles, can be utilized in the structure of micro/nanorobots.[134,135] Construction of micro/nanorobots using materials derived from patients (blood and cells) also appears as an ideal strategy to mitigate the immune response.[126,136,137]

In the stage of micro/nanorobot administration, motion sources require assessment in terms of safety. While toxic $H_2O_2$ was a standard fuel at the beginning of research, fuel-free external fields have been the primary source of motion as the research progressed in this area. Still, there can be limitations particular to each external field. For example, static magnetic fields up to 8 Tesla (T) are considered safe for medical use.[138] Although the required magnetic field strength for micro/nanorobot locomotion is negligible compared to the safe limit, the rate of change in gradient fields needs optimization due to the possibility of causing damage by heating the tissue.[139] As another promising external field, acoustic waves are generally considered to have limited damage to the tissue.[66] For light-driven micro/nanorobots, wavelength of the light source is the most determining factor in terms of safety. This limitation prevents the use of UV light in biomedical applications since it can induce severe complications. NIR light seems as the most promising light source; however, proper measures should be taken regarding power and exposure time.

Moreover, the post-treatment stage should not be overlooked since the long-term presence of non-degradable micro/nanorobots may lead to acute and chronic toxicity, potentially requiring surgical revisions.[3] To minimize long-term risks, micro/nanorobots should provide a reliable clearance strategy after completing the intended task. A safe clearance strategy can be based on degradability into non-toxic products by pH-, temperature-, and/or enzyme-triggered reactions.[87] On the other hand, this strategy does not apply to all types of micro/nanorobots given the widespread usage of non-degradable particles and coatings. As an alternative strategy, micro/nanorobots can be retrieved *via* external forces, like utilizing magnetic catheters to collect magnetically responsive microrobots.[140]

### 8.2. Fabrication

The current design of micro/nanorobots generally allows fabrication that can only be adequate for testing in laboratory conditions. This situation can be mainly related to the requirement of successive treatments and/or specific coatings attained with physical deposition methods.[141] To provide reliable solutions in daily medical treatments, large-scale fabrication techniques are highly needed. While providing high production rates, these techniques should also ensure reproducibility and cost-effectiveness. In this regard, one-step chemical synthesis techniques can be appealing for micro/nanorobots having a simple design. In other respects, intricate structures require more advanced fabrication techniques since even small alterations can cause malfunction and/or poor performance, eventually decreasing efficacy of the treatment.[87] 3D printing can be a valuable option since it ensures high resolution and uniformity for complex structures.[142–144] As significant drawbacks, the low production speed and the limited number of inks still necessitate improvements. Overall, by considering pros and cons, fabrication techniques should be an integral part of the design process to provide the most advanced micro/nanorobots in a cost-effective and reliable way.

### 8.3. Size

Micro/nanorobot size is a significant consideration due to the risk of causing occlusions in the access route before reaching the target locations. Additionally, penetrability into specific tissues can be needed for some biomedical applications, *e.g.*, targeted drug delivery to tumors. These requirements can highlight nanorobots as more effective candidates for biomedical applications rather than microrobots. On the other hand, miniaturization does not necessarily mean advanced performance regarding other functions of robots under *in vivo conditions*. For instance, blood can hinder the locomotion of robots, especially when they possess a small size (<10 μm) and/or require chemical fuels.[66] External power sources -like magnetic fields- can provide a more powerful force for locomotion. However, the miniaturization of robots also means lower magnetization due to the volume, which leads to the requirement for stronger magnetic fields.[87] Moreover, the inadequacy of imaging modalities for real-time tracking of nanorobots is a significant challenge. Related to these limitations, collective behavior of nanorobots can provide a potential remedy. With more research on this topic, nanorobotic applications can be facilitated in real-world conditions.

### 8.4. Actuation methods

A variety of physical, chemical, and biological barriers are naturally present in the body.[90,144] Although these barriers can ensure effective protection from harmful agents, they can also restrict or block micro/nanorobot locomotion. Generally, providing sufficient propulsive force and ensuring compatibility with the body can be considered as the compulsory requirements for motion sources of micro/nanorobots. In addition, every motion source can have specific pros and cons that vary with conditions of the application area. For chemically powered micro/nanorobots, self-propulsion is a significant advantage compared to externally controlled counterparts. On the other hand, they can be inadequate for applications requiring long-range locomotion, and degradation by-products can pose risks to the surrounding tissue. Also, considering the limited controllability of chemically powered micro/nanorobots, most of the recent studies utilized external power sources for locomotion. As the most widely used actuation method, magnetic fields enable robust and precisely controllable motion without a compromise even in high penetration depths.[10,145] However, the need for tracking and manipulation causes a lesser degree of autonomy *in vivo*. Related to these drawbacks, magnetically controllable biohybrid micro/nanorobots can be considered as attractive self-motile platforms.[146–149] In this approach, it is possible to enhance the availability of micro/nanorobots at target locations without requiring continuous manipulation and/or real-time tracking during the application. The need for bulky custom-built equip-

 This journal is © The Royal Society of Chemistry 2023

Published on 27 April 2023. Downloaded on 4/10/2026 3:20:11 AM.

ment can also be considered as a vital issue complicating the translation of magnetic microrobots to the clinic. The currently used systems in hospitals, such as magnetic resonance imaging (MRI) scanners, can be modified to overcome this limitation.[150] By doing so, magnetic micro/nanorobots can be more widely available for medical interventions with a cost-effective approach.

Acoustic manipulation is another noteworthy actuation method for micro/nanorobots.[151] Like magnetic fields, acoustic waves enable high-precision external motion control with minimal damage to the surrounding tissue. However, recent studies have not utilized this method adequately, which can be related to the limited number of materials responsive to acoustic waves.[142] In order to exploit the high-precision manipulation capability in deep tissues, more efforts should be devoted to the construction of acoustically actuated micro/nanorobots. Light irradiation can also be considered as a potent motion source in the micro/nanorobotic field. On the other hand, the low penetration depth is the limiting factor for this stimulus' application in the body. As a potential remedy, light sources can be combined with catheters for transmitting light to the target locations, which can pave the way for locomotion without depending on light's penetrability in the tissue.[74,152]

### 8.5. Imaging

*In vivo* imaging requires particular attention given that the recent studies mostly utilized externally driven micro/nanorobots for biomedical applications. Since these micro/nanorobots reach the target locations *via* external manipulation, convenient imaging modalities need to be incorporated during the application to receive feedback for real-time location and potential locomotion routes.[8,153] In this regard, some of the micro/nanorobots can provide advantages thanks to substrate materials' intrinsic properties. For example, different microalgae species emit fluorescence signals as an inherent functionality, and this autofluorescence property can enable *in vivo* microrobot tracking without requiring any modifications.[154] However, most of the micro/nanorobots do not hold this functionality, and this situation can lead to the need of specific contrast agents, *e.g.*, iodine- and barium-based compounds, and/or swarming behavior to more easily discriminate them from the surrounding environment.[155–157] Additionally, combining different imaging modalities can be an attractive approach to overcome limitations of the currently used modalities, *e.g.*, CT, MRI, US, PET, and SPECT.[135,158] Considering that most of the externally driven micro/nanorobots would be "blind" in the body without convenient imaging modalities, an effective approach for *in vivo* tracking should be an integral part of the micro/nanorobot design to enable the successful completion of their intended use.

## 9. Conclusion

In this review, we presented the current status of micro/nanorobotic treatments by focusing on the preclinical studies conducted with animal models. The pioneering studies discussed throughout the review have indicated promising results for different biomedical applications thanks to the active locomotion of micro/nanorobots. In various organs and body parts, micro/nanorobots have enabled localized therapies and minimally invasive operations with semi or full autonomy. Although there are significant challenges to overcome, the promise of micro/nanorobots is evident toward enhancing the efficacy of passive treatment platforms. With unique approaches provided by interdisciplinary collaborative efforts, we envision a bright future for "tiny surgeons" in a wide range of applications in daily medical use.

## Conflicts of interest

The authors declare no conflict of interest.

## Acknowledgements

M. P. acknowledges the financial support of Grant Agency of the Czech Republic (EXPRO: 19-26896X). C. M. O. acknowledges the grant CEITEC-K-21-7049 implemented within the Quality Internal Grants of BUT (Reg. No. CZ.02.2.69/0.0/0.0/19_073/0016948). The authors thank Dr. M. Ussia and Dr. M. Urso for scientific discussions.

## References

1 H. Ceylan, J. Giltinan, K. Kozielski and M. Sitti, *Lab Chip*, 2017, **17**, 1705–1724.
2 P. L. Venugopalan, B. Esteban-Fernández De Ávila, M. Pal, A. Ghosh and J. Wang, *ACS Nano*, 2020, **14**, 9423–9439.
3 H. Ceylan, I. C. Yasa, U. Kilic, W. Hu and M. Sitti, *Prog. Biomed. Eng.*, 2019, **1**, 012002.
4 M. Urso and M. Pumera, *Adv. Funct. Mater.*, 2022, **32**, 2200711.
5 W. Wang and C. Zhou, *Adv. Healthcare Mater.*, 2021, **10**, 2001236.
6 X. Liu, X. Sun, Y. Peng, Y. Wang, D. Xu, W. Chen, W. Wang, X. Yan and X. Ma, *ACS Nano*, 2022, **16**, 14666–14678.
7 J. Li, B. E. F. De Ávila, W. Gao, L. Zhang and J. Wang, *Sci. Robot.*, 2017, **2**, eaam6431.
8 M. Sun, K. F. Chan, Z. Zhang, L. Wang, Q. Wang, S. Yang, S. M. Chan, P. W. Y. Chiu, J. J. Y. Sung and L. Zhang, *Adv. Mater.*, 2022, **34**, 2201888.
9 H. W. Huang, F. E. Uslu, P. Katsamba, E. Lauga, M. S. Sakar and B. J. Nelson, *Sci. Adv.*, 2019, **5**, eaau1532.
10 Y. Dong, L. Wang, Z. Zhang, F. Ji, T. K. F. Chan, H. Yang, C. P. L. Chan, Z. Yang, Z. Chen, W. T. Chang, J. Y. K. Chan, J. J. Y. Sung and L. Zhang, *Sci. Adv.*, 2022, **8**, eabq8573.
11 M. Wan, Q. Wang, Q. Wang, R. Wang, R. Wu, T. Li, D. Fang, Y. Huang, Y. Yu, L. Fang, X. Wang, Y. Zhang,

Published on 27 April 2023. Downloaded on 4/10/2026 3:20:11 AM.

Z. Miao, B. Zhao, F. Wang, C. Mao, Q. Jiang, X. Xu and D. Shi, *Sci. Adv.*, 2020, **6**, eaaz9014.
12 M. Ussia, M. Urso, S. Kment, T. Fialova, K. Klima, K. Dolezelikova and M. Pumera, *Small*, 2022, **18**, 2200708.
13 H. Choi, B. Kim, S. H. Jeong, T. Y. Kim, D. Kim, Y. Oh and S. K. Hahn, *Small*, 2022, 2204617.
14 J. Zheng, W. Wang, X. Gao, S. Zhao, W. Chen, J. Li and Y. N. Liu, *Small*, 2022, 2205252.
15 C. C. Mayorga-Martinez, J. Zelenka, K. Klima, P. Mayorga-Burrezo, L. Hoang, T. Ruml and M. Pumera, *ACS Nano*, 2022, **16**, 8694–8703.
16 H. Zhang, Z. Li, C. Gao, X. Fan, Y. Pang, T. Li, Z. Wu, H. Xie and Q. He, *Sci. Robot.*, 2020, **6**, eaaz9519.
17 A. V. Singh, M. H. Dad Ansari, C. B. Dayan, J. Giltinan, S. Wang, Y. Yu, V. Kishore, P. Laux, A. Luch and M. Sitti, *Biomaterials*, 2019, **219**, 119394.
18 Z. Jin, K. T. Nguyen, G. Go, B. Kang, H. K. Min, S. J. Kim, Y. Kim, H. Li, C. S. Kim, S. Lee, S. Park, K. P. Kim, K. M. Huh, J. Song, J. O. Park and E. Choi, *Nano Lett.*, 2019, **19**, 8550–8564.
19 Q. Fu, H. Feng, L. Liu, Z. Li, J. Li, J. Hu, C. Hu, X. Yan, H. Yang and J. Song, *Angew. Chem., Int. Ed.*, 2022, **61**, e202213319.
20 M. M. Wan, H. Chen, Z. Da Wang, Z. Y. Liu, Y. Q. Yu, L. Li, Z. Y. Miao, X. W. Wang, Q. Wang, C. Mao, J. Shen and J. Wei, *Adv. Sci.*, 2021, **8**, 2002525.
21 A. Aghakhani, A. Pena-Francesch, U. Bozuyuk, H. Cetin, P. Wrede and M. Sitti, *Sci. Adv.*, 2022, **8**, eabm5126.
22 L. Zhang, B. Zhang, R. Liang, H. Ran, D. Zhu, J. Ren, L. Liu, A. Ma and L. Cai, *ACS Nano*, 2023, **17**, 6410–6422.
23 K. Chen, X. Peng, M. Dang, J. Tao, J. Ma, Z. Li, L. Zheng, X. Su, L. Wang and Z. Teng, *ACS Appl. Mater. Interfaces*, 2021, **13**, 51297–51311.
24 S. Wang, K. Liu, Q. Zhou, C. Xu, J. Gao, Z. Wang, F. Wang, B. Chen, Y. Ye, J. Ou, J. Jiang, D. A. Wilson, S. Liu, F. Peng and Y. Tu, *Adv. Funct. Mater.*, 2021, **31**, 2009475.
25 Q. Song, X. Ding, Y. Liu, W. Liu, J. Li, B. Wang and Z. Gu, *Appl. Mater. Today*, 2023, **31**, 101779.
26 K. Ariga, J. Li, J. Fei, Q. Ji and J. P. Hill, *Adv. Mater.*, 2016, **28**, 1251–1286.
27 A. Jancik-Prochazkova, H. Michalkova, Z. Heger and M. Pumera, *ACS Nano*, 2023, **17**, 146–156.
28 Y. Xing, M. Zhou, X. Liu, M. Qiao, L. Zhou, T. Xu, X. Zhang and X. Du, *Chem. Eng. J.*, 2023, **461**, 142142.
29 K. Ariga, *Chem. Sci.*, 2020, **11**, 10594–10604.
30 J. Li, P. Angsantikul, W. Liu, B. Esteban-Fernández de Ávila, S. Thamphiwatana, M. Xu, E. Sandraz, X. Wang, J. Delezuk, W. Gao, L. Zhang and J. Wang, *Angew. Chem., Int. Ed.*, 2017, **56**, 2156–2161.
31 B. Esteban-Fernández de Ávila, P. Angsantikul, J. Li, W. Gao, L. Zhang and J. Wang, *Adv. Funct. Mater.*, 2018, **28**, 1705640.
32 R. Mundaca-Uribe, B. Esteban-Fernández de Ávila, M. Holay, P. Lekshmy Venugopalan, B. Nguyen, J. Zhou, A. Abbas, R. H. Fang, L. Zhang and J. Wang, *Adv. Healthcare Mater.*, 2020, **9**, 2000900.
33 C. Wang, B. E. Fernández de Ávila, R. Mundaca-Uribe, M. A. Lopez-Ramirez, D. E. Ramírez-Herrera, S. Shukla, N. F. Steinmetz and J. Wang, *Small*, 2020, **16**, 1907150.
34 F. Zhang, Z. Li, L. Yin, Q. Zhang, N. Askarinam, R. Mundaca-Uribe, F. Tehrani, E. Karshalev, W. Gao, L. Zhang and J. Wang, *J. Am. Chem. Soc.*, 2021, **143**, 12194–12201.
35 J. Zhou, E. Karshalev, R. Mundaca-Uribe, B. Esteban-Fernández de Ávila, N. Krishnan, C. Xiao, C. J. Ventura, H. Gong, Q. Zhang, W. Gao, R. H. Fang, J. Wang and L. Zhang, *Adv. Mater.*, 2021, **33**, 2103505.
36 L. Cai, C. Zhao, H. Chen, L. Fan, Y. Zhao, X. Qian and R. Chai, *Adv. Sci.*, 2021, **9**, 2103384.
37 K. Liu, Q. Liu, J. Yang, C. Xie, S. Wang, F. Tong, J. Gao, L. Liu, Y. Ye, B. Chen, X. Cai, Z. Liu, Z. Li, F. Peng and Y. Tu, *ACS Nano*, 2022, **17**, 300–311.
38 Q. Li, L. Liu, H. Huo, L. Su, Y. Wu, H. Lin, X. Ge, J. Mu, X. Zhang, L. Zheng and J. Song, *ACS Nano*, 2022, **16**, 7947–7960.
39 S. Zhang, J. Chen, M. L. Lian, W. S. Yang and X. Chen, *Chem. Eng. J.*, 2022, **446**, 136794.
40 M. Valles, S. Pujals, L. Albertazzi and S. Sánchez, *ACS Nano*, 2022, **16**, 5615–5626.
41 Z. Chen, T. Xia, Z. Zhang, S. Xie, T. Wang and X. Li, *Chem. Eng. J.*, 2019, **375**, 122109.
42 H. Choi, S. H. Cho and S. K. Hahn, *ACS Nano*, 2020, **14**, 6683–6692.
43 B. Zhang, H. Pan, Z. Chen, T. Yin, M. Zheng and L. Cai, *Sci. Adv.*, 2023, **9**, eadc8978.
44 H. Tian, J. Ou, Y. Wang, J. Sun, J. Gao, Y. Ye, R. Zhang, B. Chen, F. Wang, W. Huang, H. Li, L. Liu, C. Shao, Z. Xu, F. Peng and Y. Tu, *Acta Pharm. Sin. B*, DOI: **10.1016/j.apsb.2023.02.016**.
45 V. Magdanz, I. S. M. Khalil, J. Simmchen, G. P. Furtado, S. Mohanty, J. Gebauer, H. Xu, A. Klingner, A. Aziz, M. Medina-Sánchez, O. G. Schmidt and S. Misra, *Sci. Adv.*, 2020, **6**, eaba5855.
46 J. Xing, T. Yin, S. Li, T. Xu, A. Ma, Z. Chen, Y. Luo, Z. Lai, Y. Lv, H. Pan, R. Liang, X. Wu, M. Zheng and L. Cai, *Adv. Funct. Mater.*, 2021, **31**, 2008262.
47 F. Zhang, Z. Li, Y. Duan, H. Luan, L. Yin, Z. Guo, C. Chen, M. Xu, W. Gao, R. H. Fang, L. Zhang and J. Wang, *Sci. Adv.*, 2022, **8**, eade6455.
48 Y. Alapan, O. Yasa, B. Yigit, I. C. Yasa, P. Erkoc and M. Sitti, *Annu. Rev. Control. Robot. Auton. Syst.*, 2019, **2**, 205–230.
49 M. Urso, M. Ussia and M. Pumera, *Nat. Rev. Bioeng.*, 2023, **1**, 236–251.
50 H. Wang and M. Pumera, *Adv. Funct. Mater.*, 2018, **28**, 1705421.
51 X. Peng, M. Urso, J. Balvan, M. Masarik and M. Pumera, *Angew. Chem., Int. Ed.*, 2022, **61**, e202213505.
52 Y. Zu, Y. Yong, X. Zhang, J. Yu, X. Dong, W. Yin, L. Yan, F. Zhao, Z. Gu and Y. Zhao, *RSC Adv.*, 2017, **7**, 17505–17513.
53 X. Zhang, G. Chen, X. Fu, Y. Wang and Y. Zhao, *Adv. Mater.*, 2021, **33**, 2104932.

 This journal is © The Royal Society of Chemistry 2023

Published on 27 April 2023. Downloaded on 4/10/2026 3:20:11 AM.

54 T. Wei, J. Liu, D. Li, S. Chen, Y. Zhang, J. Li, L. Fan, Z. Guan, C. M. Lo, L. Wang, K. Man and D. Sun, *Small*, 2020, **16**, 1906908.
55 M. Hoop, A. S. Ribeiro, D. Rösch, P. Weinand, N. Mendes, F. Mushtaq, X. Z. Chen, Y. Shen, C. F. Pujante, J. Puigmartí-Luis, J. Paredes, B. J. Nelson, A. P. Pêgo and S. Pané, *Adv. Funct. Mater.*, 2018, **28**, 1705920.
56 A. Servant, F. Qiu, M. Mazza, K. Kostarelos and B. J. Nelson, *Adv. Mater.*, 2015, **27**, 2981–2988.
57 K. Hou, Y. Zhang, M. Bao, C. Xin, Z. Wei, G. Lin and Z. Wang, *ACS Appl. Mater. Interfaces*, 2022, **14**, 3825–3837.
58 M. Ussia, M. Urso, M. Kratochvilova, J. Navratil, J. Balvan, C. C. Mayorga-Martinez, J. Vyskocil, M. Masarik and M. Pumera, *Small*, 2023, 2208259.
59 D. Zhong, W. Li, Y. Qi, J. He and M. Zhou, *Adv. Funct. Mater.*, 2020, **30**, 1910395.
60 H. Zhang, Z. Li, Z. Wu and Q. He, *Adv. Ther.*, 2019, **2**, 1900096.
61 C. Dillinger, N. Nama and D. Ahmed, *Nat. Commun.*, 2021, **12**, 6455.
62 J. Li, C. C. Mayorga-Martinez, C. Ohl and M. Pumera, *Adv. Funct. Mater.*, 2021, **32**, 2102265.
63 J. Ye, Q. Fu, L. Liu, L. Chen, X. Zhang, Q. Li, Z. Li, L. Su, R. Zhu, J. Song and H. Yang, *Sci. China: Chem.*, 2021, **64**, 2218–2229.
64 A. D. C. Fonseca, C. Glück, J. Droux, Y. Ferry, C. Frei, S. Wegener, B. Weber, M. El Amki and D. Ahmed, *bioRxiv*, 2023, DOI: **10.1101/2023.01.28.522839**.
65 C. M. Oral, M. Ussia, D. K. Yavuz and M. Pumera, *Small*, 2022, **18**, 2106271.
66 M. Wan, T. Li, H. Chen, C. Mao and J. Shen, *Angew. Chem., Int. Ed.*, 2021, **60**, 13158–13176.
67 V. Sridhar, E. Yildiz, A. Rodríguez-Camargo, X. Lyu, L. Yao, P. Wrede, A. Aghakhani, B. M. Akolpoglu, F. Podjaski, B. V. Lotsch and M. Sitti, *Adv. Mater.*, DOI: **10.1002/adma.202301126**.
68 Y. Liu, G. Lin, G. Bao, M. Guan, L. Yang, Y. Liu, D. Wang, X. Zhang, J. Liao, G. Fang, X. Di, G. Huang, J. Zhou, Y. Y. Cheng and D. Jin, *ACS Nano*, 2021, **15**, 19924–19937.
69 C. M. Oral, M. Ussia and M. Pumera, *Small*, 2022, **18**, 2202600.
70 M. J. Oh, A. Babeer, Y. Liu, Z. Ren, J. Wu, D. A. Issadore, K. J. Stebe, D. Lee, E. Steager and H. Koo, *ACS Nano*, 2022, **16**, 11998–12012.
71 E. Karshalev, Y. Zhang, B. Esteban-Fernández De Ávila, M. Beltrán-Gastélum, Y. Chen, R. Mundaca-Uribe, F. Zhang, B. Nguyen, Y. Tong, R. H. Fang, L. Zhang and J. Wang, *Nano Lett.*, 2019, **19**, 7816–7826.
72 H. Wang, X. Chen, Y. Qi, C. Wang, L. Huang, R. Wang, J. Li, X. Xu, Y. Zhou, Y. Liu and X. Xue, *Adv. Mater.*, 2022, **34**, 2206779.
73 F. Zhang, J. Zhuang, Z. Li, H. Gong, B. E. F. de Ávila, Y. Duan, Q. Zhang, J. Zhou, L. Yin, E. Karshalev, W. Gao, V. Nizet, R. H. Fang, L. Zhang and J. Wang, *Nat. Mater.*, 2022, **21**, 1324–1332.
74 J. Wang, F. Soto, S. Liu, Q. Yin, E. Purcell, Y. Zeng, E. C. Hsu, D. Akin, B. Sinclair, T. Stoyanova and U. Demirci, *Adv. Funct. Mater.*, 2022, **32**, 2201800.
75 L. Xie, X. Pang, X. Yan, Q. Dai, H. Lin, J. Ye, Y. Cheng, Q. Zhao, X. Ma, X. Zhang, G. Liu and X. Chen, *ACS Nano*, 2020, **14**, 2880–2893.
76 W. Cao, Y. Liu, P. Ran, J. He, S. Xie, J. Weng and X. Li, *ACS Appl. Mater. Interfaces*, 2021, **13**, 58411–58421.
77 M. Wan, Q. Wang, X. Li, B. Xu, D. Fang, T. Li, Y. Yu, L. Fang, Y. Wang, M. Wang, F. Wang, C. Mao, J. Shen and J. Wei, *Angew. Chem., Int. Ed.*, 2020, **59**, 14458–14465.
78 W. Gao, R. Dong, S. Thamphiwatana, J. Li, W. Gao, L. Zhang and J. Wang, *ACS Nano*, 2015, **9**, 117–123.
79 B. Esteban-Fernández de Ávila, M. A. Lopez-Ramirez, R. Mundaca-Uribe, X. Wei, D. E. Ramírez-Herrera, E. Karshalev, B. Nguyen, R. H. Fang, L. Zhang and J. Wang, *Adv. Mater.*, 2020, **32**, 2000091.
80 B. E. F. De Ávila, P. Angsantikul, J. Li, M. A. Lopez-Ramirez, D. E. Ramírez-Herrera, S. Thamphiwatana, C. Chen, J. Delezuk, R. Samakapiruk, V. Ramez, L. Zhang and J. Wang, *Nat. Commun.*, 2017, **8**, 272.
81 E. Karshalev, B. Esteban-Fernández De Ávila, M. Beltrán-Gastélum, P. Angsantikul, S. Tang, R. Mundaca-Uribe, F. Zhang, J. Zhao, L. Zhang and J. Wang, *ACS Nano*, 2018, **12**, 8397–8405.
82 J. Li, S. Thamphiwatana, W. Liu, B. Esteban-Fernández De Ávila, P. Angsantikul, E. Sandraz, J. Wang, T. Xu, F. Soto, V. Ramez, X. Wang, W. Gao, L. Zhang and J. Wang, *ACS Nano*, 2016, **10**, 9536–9542.
83 X. Wei, M. Beltrán-Gastélum, E. Karshalev, B. Esteban-Fernández De Ávila, J. Zhou, D. Ran, P. Angsantikul, R. H. Fang, J. Wang and L. Zhang, *Nano Lett.*, 2019, **19**, 1914–1921.
84 Z. Wu, L. Li, Y. Yang, P. Hu, Y. Li, S. Y. Yang, L. V. Wang and W. Gao, *Sci. Robot.*, 2019, **4**, eaax0613.
85 Z. Wang, M. Chu, N. Yin, W. Huang and W. Liu, *Sci. Adv.*, 2022, **8**, eabn3917.
86 F. Zhang, Z. Li, Y. Duan, A. Abbas, R. Mundaca-Uribe, L. Yin, H. Luan, W. Gao, R. H. Fang, L. Zhang and J. Wang, *Sci. Robot.*, 2022, **7**, eabo4160.
87 C. K. Schmidt, M. Medina-Sánchez, R. J. Edmondson and O. G. Schmidt, *Nat. Commun.*, 2020, **11**, 5618.
88 G. Go, A. Yoo, K. T. Nguyen, M. Nan, B. A. Darmawan, S. Zheng, B. Kang, C. S. Kim, D. Bang, S. Lee, K. P. Kim, S. S. Kang, K. M. Shim, S. E. Kim, S. Bang, D. H. Kim, J. O. Park and E. Choi, *Sci. Adv.*, 2022, **8**, eabq8545.
89 Y. Dai, X. Bai, L. Jia, H. Sun, Y. Feng, L. Wang, C. Zhang, Y. Chen, Y. Ji, D. Zhang, H. Chen and L. Feng, *Small*, 2021, **17**, 2103986.
90 J. R. Baylis, J. H. Yeon, M. H. Thomson, A. Kazerooni, X. Wang, A. E. S. John, E. B. Lim, D. Chien, A. Lee, J. Q. Zhang, J. M. Piret, L. S. Machan, T. F. Burke, N. J. White and C. J. Kastrup, *Sci. Adv.*, 2015, **1**, e1500379.
91 Q. Li, E. Hu, K. Yu, R. Xie, F. Lu, B. Lu, R. Bao, T. Zhao, F. Dai and G. Lan, *Adv. Funct. Mater.*, 2020, **30**, 2004153.

Published on 27 April 2023. Downloaded on 4/10/2026 3:20:11 AM.

92 E. Gultepe, J. S. Randhawa, S. Kadam, S. Yamanaka, F. M. Selaru, E. J. Shin, A. N. Kalloo and D. H. Gracias, *Adv. Mater.*, 2013, **25**, 514–519.
93 A. C. Hortelao, R. Carrascosa, N. Murillo-Cremaes, T. Patino and S. Sánchez, *ACS Nano*, 2019, **13**, 429–439.
94 X. Zhang, T. Yang, Y. Wu and Q. He, *Nanoscale*, 2022, **14**, 12547–12559.
95 Z. Cong, S. Tang, L. Xie, M. Yang, Y. Li, D. Lu, J. Li, Q. Yang, Q. Chen, Z. Zhang, X. Zhang and S. Wu, *Adv. Mater.*, 2022, **34**, 2201042.
96 A. Aziz, J. Holthof, S. Meyer, O. G. Schmidt and M. Medina-Sánchez, *Adv. Healthcare Mater.*, 2021, **10**, 2101077.
97 A. C. Hortelao, C. Simó, M. Guix, S. Guallar-Garrido, E. Julián, D. Vilela, L. Rejc, P. Ramos-Cabrer, U. Cossío, V. Gómez-Vallejo, T. Patiño, J. Llop and S. Sánchez, *Sci. Robot.*, 2021, **6**, eabd2823.
98 J. Yoo, S. Tang and W. Gao, *Nat. Rev. Bioeng.*, DOI: 10.1038/s44222-023-00038-4.
99 G. Deng, X. Peng, Z. Sun, W. Zheng, J. Yu, L. Du, H. Chen, P. Gong, P. Zhang, L. Cai and B. Z. Tang, *ACS Nano*, 2020, **14**, 11452–11462.
100 A. Joseph, C. Contini, D. Cecchin, S. Nyberg, L. Ruiz-Perez, J. Gaitzsch, G. Fullstone, X. Tian, J. Azizi, J. Preston, G. Volpe and G. Battaglia, *Sci. Adv.*, 2017, **3**, e1700362.
101 S. Jeon, S. H. Park, E. Kim, J. Kim, S. W. Kim and H. Choi, *Adv. Healthcare Mater.*, 2021, **10**, 2100801.
102 P. Wrede, O. Degtyaruk, S. K. Kalva, X. L. Deán-ben, U. Bozuyuk, A. Aghakhani, B. Akolpoglu, M. Sitti and D. Razansky, *Sci. Adv.*, 2022, **8**, eabm9132.
103 R. Cheng, W. Huang, L. Huang, B. Yang, L. Mao, K. Jin, Q. Zhuge and Y. Zhao, *ACS Nano*, 2014, **8**, 7746–7754.
104 J. Hu, S. Huang, L. Zhu, W. Huang, Y. Zhao, K. Jin and Q. Zhuge, *ACS Appl. Mater. Interfaces*, 2018, **10**, 32988–32997.
105 X. Tang, L. Manamanchaiyaporn, Q. Zhou, C. Huang, L. Li, Z. Li, L. Wang, J. Wang, L. Ren, T. Xu, X. Yan and Y. Zheng, *Small*, 2022, **18**, 2202848.
106 S. Xie, S. Li, W. Cao, C. Mo, Z. Zhang, K. Huang and X. Li, *ACS Appl. Mater. Interfaces*, 2022, **14**, 37553–37565.
107 L. Wang, J. Wang, J. Hao, Z. Dong, J. Wu, G. Shen, T. Ying, L. Feng, X. Cai, Z. Liu and Y. Zheng, *Adv. Mater.*, 2021, **33**, 2105351.
108 Q. Deng, L. Zhang, W. Lv, X. Liu, J. Ren and X. Qu, *ACS Nano*, 2021, **15**, 6604–6613.
109 Y. Huang, T. Li, W. Gao, Q. Wang, X. Li, C. Mao, M. Zhou, M. Wan and J. Shen, *J. Mater. Chem. B*, 2020, **8**, 5765–5775.
110 J. Law, X. Wang, M. Luo, L. Xin, X. Du, W. Dou, T. Wang, G. Shan, Y. Wang, P. Song, X. Huang, J. Yu and Y. Sun, *Sci. Adv.*, 2022, **8**, eabm5752.
111 Z. Wu, J. Troll, H. H. Jeong, Q. Wei, M. Stang, F. Ziemssen, Z. Wang, M. Dong, S. Schnichels, T. Qiu and P. Fischer, *Sci. Adv.*, 2018, **4**, eaat4388.
112 G. Chatzipirpiridis, O. Ergeneman, J. Pokki, F. Ullrich, S. Fusco, J. A. Ortega, K. M. Sivaraman, B. J. Nelson and S. Pané, *Adv. Healthcare Mater.*, 2015, **4**, 209–214.
113 J. Pokki, O. Ergeneman, S. Sevim, V. Enzmann, H. Torun and B. J. Nelson, *Biomed. Microdevices*, 2015, **17**, 85.
114 J. Pokki, O. Ergeneman, G. Chatzipirpiridis, T. Lühmann, J. Sort, E. Pellicer, S. A. Pot, B. M. Spiess, S. Pané and B. J. Nelson, *J. Biomed. Mater. Res., Part B*, 2017, **105**, 836–845.
115 F. Ullrich, C. Bergeles, J. Pokki, O. Ergeneman, S. Erni, G. Chatzipirpiridis, S. Pané, C. Framme and B. J. Nelson, *Invest. Ophthalmol. Visual Sci.*, 2013, **54**, 2853–2863.
116 W. He, J. Frueh, N. Hu, L. Liu, M. Gai and Q. He, *Adv. Sci.*, 2016, **3**, 1600206.
117 S. Xie, K. Huang, J. Peng, Y. Liu, W. Cao, D. Zhang, X. Li, S. Xie, K. Huang, J. W. Peng, Y. Liu, W. X. Cao, D. D. Zhang and X. H. Li, *Adv. Healthcare Mater.*, 2022, **11**, 2201323.
118 X. Arque, M. D. Torres, T. Patino, A. Boaro, S. Sanchez and C. de la Fuente-Nunez, *ACS Nano*, 2022, **16**, 7547–7558.
119 C. Xu, Y. Liu, J. Li, P. Ning, Z. Shi, W. Zhang, Z. Li, R. Zhou, Y. Tong, Y. Li, C. Lv, Y. Shen, Q. Cheng, B. He and Y. Cheng, *Adv. Mater.*, 2023, **35**, 2204996.
120 H. Zhong, Z. Zhang, Y. Zhou, L. Wu, P. Ke, Y. Lu, Q. Dai, X. Bao, Y. Xia, Q. Yang, X. Tan, Q. Wei, W. Xu, M. Han and L. Ma, *ACS Appl. Mater. Interfaces*, 2022, **14**, 38172–38184.
121 V. Du Nguyen, H. K. Min, H. Y. Kim, J. Han, Y. H. Choi, C. S. Kim, J. O. Park and E. Choi, *ACS Nano*, 2021, **15**, 8492–8506.
122 J. Ren, P. Hu, E. Ma, X. Zhou, W. Wang, S. Zheng and H. Wang, *Appl. Mater. Today*, 2022, **27**, 101445.
123 W. Chen, R. Jiang, X. Sun, S. Chen, X. Liu, M. Fu, X. Yan and X. Ma, *Chem. Mater.*, 2022, **34**, 7543–7552.
124 Y. Xing, J. Xiu, M. Zhou, T. Xu, M. Zhang, H. Li, X. Li, X. Du, T. Ma and X. Zhang, *ACS Nano*, 2023, **17**, 6789–6799.
125 X. Tang, Y. Yang, M. Zheng, T. Yin, G. Huang, Z. Lai, B. Zhang, Z. Chen, T. Xu, T. Ma, H. Pan and L. Cai, *Adv. Mater.*, 2023, 2211509.
126 L. Yue, C. Gao, J. Li, H. Chen, S. M. Y. Lee, R. Luo and R. Wang, *Adv. Mater.*, 2023, 2211626.
127 Y. Zhang, K. Zhang, H. Yang, Y. Hao, J. Zhang, W. Zhao, S. Zhang, S. Ma and C. Mao, *ACS Appl. Mater. Interfaces*, 2023, **15**, 14099–14110.
128 L. Liu, J. Wu, B. Chen, J. Gao, T. Li, Y. Ye, H. Tian, S. Wang, F. Wang, J. Jiang, J. Ou, F. Tong, F. Peng and Y. Tu, *ACS Nano*, 2022, **16**, 6515–6526.
129 C. Xu, S. Wang, H. Wang, K. Liu, S. Zhang, B. Chen, H. Liu, F. Tong, F. Peng, Y. Tu and Y. Li, *Nano Lett.*, 2021, **21**, 1982–1991.
130 Y. Zhao, H. Xiong, Y. Li, W. Gao, C. Hua, J. Wu, C. Fan, X. Cai and Y. Zheng, *Adv. Intell. Syst.*, 2022, **4**, 2200061.
131 G. Go, S. G. Jeong, A. Yoo, J. Han, B. Kang, S. Kim, K. T. Nguyen, Z. Jin, C. S. Kim, Y. R. Seo, J. Y. Kang, J. Y. Na, E. K. Song, Y. Jeong, J. K. Seon, J. O. Park and E. Choi, *Sci. Robot.*, 2020, **5**, eaay6626.
132 R. Nauber, S. R. Goudu, M. Goeckenjan, M. Bornhäuser, C. Ribeiro and M. Medina-Sánchez, *Nat. Commun.*, 2023, **14**, 728.

 This journal is © The Royal Society of Chemistry 2023

Published on 27 April 2023. Downloaded on 4/10/2026 3:20:11 AM.

133 I. C. Yasa, A. F. Tabak, O. Yasa, H. Ceylan and M. Sitti, *Adv. Funct. Mater.*, 2019, **29**, 1808992.
134 U. Bozuyuk, E. Suadiye, A. Aghakhani, N. O. Dogan, J. Lazovic, M. E. Tiryaki, M. Schneider, A. C. Karacakol, S. O. Demir, G. Richter and M. Sitti, *Adv. Funct. Mater.*, 2022, **32**, 2109741.
135 B. Wang, K. Kostarelos, B. J. Nelson and L. Zhang, *Adv. Mater.*, 2021, **33**, 2002047.
136 H. Ceylan, N. O. Dogan, I. C. Yasa, M. N. Musaoglu, Z. U. Kulali and M. Sitti, *Sci. Adv.*, 2021, **7**, eabh0273.
137 N. O. Dogan, H. Ceylan, E. Suadiye, D. Sheehan, A. Aydin, I. C. Yasa, A. M. Wild, G. Richter and M. Sitti, *Small*, 2022, **18**, 2204016.
138 J. F. Schenck, *J. Magn. Reson. Imaging*, 2000, **12**, 2–19.
139 P. Erkoc, I. C. Yasa, H. Ceylan, O. Yasa, Y. Alapan and M. Sitti, *Adv. Ther.*, 2019, **2**, 1800064.
140 K. T. Nguyen, G. Go, Z. Jin, B. A. Darmawan, A. Yoo, S. Kim, M. Nan, S. B. Lee, B. Kang, C. S. Kim, H. Li, D. Bang, J. O. Park and E. Choi, *Adv. Healthcare Mater.*, 2021, **10**, 2001681.
141 M. Urso and M. Pumera, *Adv. Funct. Mater.*, 2022, **32**, 2112120.
142 S. R. Dabbagh, M. R. Sarabi, M. T. Birtek, S. Seyfi, M. Sitti and S. Tasoglu, *Nat. Commun.*, 2022, **13**, 5875.
143 H. Ceylan, I. C. Yasa, O. Yasa, A. F. Tabak, J. Giltinan and M. Sitti, *ACS Nano*, 2019, **13**, 3353–3362.
144 I. C. Yasa, H. Ceylan, U. Bozuyuk, A. M. Wild and M. Sitti, *Sci. Robot.*, 2020, **5**, eaaz3867.
145 H. Zhou, C. C. Mayorga-Martinez, S. Pané, L. Zhang and M. Pumera, *Chem. Rev.*, 2021, **121**, 4999–5041.
146 T. Gwisai, N. Mirkhani, M. G. Christiansen, T. T. Nguyen, V. Ling and S. Schuerle, *Sci. Robot.*, 2022, **7**, eabo0665.
147 M. B. Akolpoglu, Y. Alapan, N. O. Dogan, S. F. Baltaci, O. Yasa, G. A. Tural and M. Sitti, *Sci. Adv.*, 2022, **8**, eabo6163.
148 H. Chen, Y. Li, Y. Wang, P. Ning, Y. Shen, X. Wei, Q. Feng, Y. Liu, Z. Li, C. Xu, S. Huang, C. Deng, P. Wang and Y. Cheng, *ACS Nano*, 2022, **16**, 6118–6133.
149 O. Felfoul, M. Mohammadi, S. Taherkhani, D. de Lanauze, Y. Z. Xu, D. Loghin, S. Essa, S. Jancik, D. Houle, M. Lafleur, L. Gaboury, M. Tabrizian, N. Kaou, M. Atkin, T. Vuong, G. Batist, N. Beauchemin, D. Radzioch and S. Martel, *Nat. Nanotechnol.*, 2016, **11**, 941–947.
150 M. E. Tiryaki and M. Sitti, *Adv. Intell. Syst.*, 2022, **4**, 2100178.
151 V. M. Jooss, J. S. Bolten, J. Huwyler and D. Ahmed, *Sci. Adv.*, 2022, **8**, eabm2785.
152 M. Sitti and D. S. Wiersma, *Adv. Mater.*, 2020, **32**, 1906766.
153 Q. Wang, K. F. Chan, K. Schweizer, X. Du, D. Jin, S. C. H. Yu, B. J. Nelson and L. Zhang, *Sci. Adv.*, 2021, **7**, eabe5914.
154 X. Yan, Q. Zhou, M. Vincent, Y. Deng, J. Yu, J. Xu, T. Xu, T. Tang, L. Bian, Y. X. J. Wang, K. Kostarelos and L. Zhang, *Sci. Robot.*, 2017, **2**, eaaq1155.
155 C. M. Oral, M. Ussia, M. Urso, J. Salat, A. Novobilsky, M. Stefanik, D. Ruzek and M. Pumera, *Adv. Healthcare Mater.*, 2023, **12**, 2202682.
156 A. Aziz, S. Pane, V. Iacovacci, N. Koukourakis, J. Czarske, A. Menciassi, M. Medina-Sánchez and O. G. Schmidt, *ACS Nano*, 2020, **14**, 10865–10893.
157 D. Dubey, M. G. Christiansen, M. Vizovisek, S. Gebhardt, J. Feike and S. Schuerle, *Small*, 2022, **2107143**, 2107143.
158 G. T. van Moolenbroek, T. Patiño, J. Llop and S. Sánchez, *Adv. Intell. Syst.*, 2020, **2**, 2000087.